THE UNIVERSITY *of* EDINBURGH

Edinburgh Research Explorer

Performance Analysis of NOMA Enabled Hybrid Network with Limited Feedback

Citation for published version:
Swami, P, Singh, MK, Bhatia, V & Ratnarajah, T 2020, 'Performance Analysis of NOMA Enabled Hybrid Network with Limited Feedback', *IEEE Transactions on Vehicular Technology*.
https://doi.org/10.1109/TVT.2020.2974004

Digital Object Identifier (DOI):
10.1109/TVT.2020.2974004

Document Version:
Peer reviewed version

Published In:
IEEE Transactions on Vehicular Technology

Performance Analysis of NOMA Enabled Hybrid Network with Limited Feedback

Pragya Swami, Mukesh Kumar Mishra, Vimal Bhatia, *Senior Member, IEEE*, and Tharmalingam Ratnarajah, *Senior Member, IEEE*

***Abstract*—This paper investigates the coexistence of multi radio access technology (RAT) using Ultra High Frequency (UHF) small base station (SBS) and millimeter Wave (mmWave) SBS tier in a heterogeneous network (HetNet). To support large number of users, non-orthogonal multiple access (NOMA) is used in the SBS tier. For NOMA, the SBS needs to obtain users' channel state information (CSI) to determine their ordering. Acquiring CSI at the SBS is a challenging task due to the massively increased number of users. The existing literature uses limited feedback from the users as a potential solution to assist the SBS in user ordering, when perfect CSI is not known at the base station. The limited feedback from the users in the existing literature is used only for user ordering. However, in the proposed work, unlike using limited feedback only for user ordering, the usage of limited feedback from the users is twofold. The first one is for the user ordering and the second is for the RAT selection. The impact of the proposed feedback system is analyzed in a NOMA enabled hybrid UHF/mmWave downlink HetNet. Numerical results show that the proposed feedback system achieves significant improvement in the outage probability.**

***Index Terms*—Non-orthogonal multiple access, mmWave, heterogeneous network, limited feedback, outage probability.**

I. Introduction

Non-orthogonal multiple access (NOMA) and millimeter wave (mmWave) communication, both have gained enormous research attention in 5G and beyond wireless networks. NOMA enhances spectral efficiency and increases the number of connected devices, while mmWave communication increases data rates by providing a very large bandwidth. However, transmissions using higher mmWave frequencies suffer from large attenuation and high sensitivity to blockages [1]. Additionally, providing initial access using beamtraining with thin beams to standalone mmWave small base stations (SBSs) is challenging [2]. If the position of ultra high frequency (UHF) SBS and mmWave-SBS (mSBS) relative to one another are known in a multi-radio access technology (RAT) heterogeneous network (HetNet), the information acquired by the UHF-SBS (uSBS) can be shared with the mSBS. This speeds up the initial access procedure, since the coarse-grained angle information for beamtraining can be derived easily using the shared information from the uSBS [2].

A. Motivation and Contribution

Proposing a future cellular network with the co-existence of multiple-RATs is a more practical approach [2]. Moreover, due to the increased load on the macro base station (MBS) tier due to rapidly increasing number of users, offloading the users to the SBS aids in load balancing in a HetNet [3]. At the SBS tier, it might not be possible to dedicate an entire frequency band to the offloaded user (OU) due to resource constraints. Motivated by the merits of NOMA, need for the co-existence of multi RAT SBSs, and the challenge of acquiring channel state information (CSI) at the SBS for large number of users, this work proposes a NOMA enabled hybrid HetNet with limited feedback. Since the channel needs to be estimated at the user, fed into a quantizer that returns a small number of feedback bits which are transmitted back to the SBS, limited feedback (using one-bit quantization technique) reduces the system overhead [4]–[6]. The major contributions of the work are as follows:

- The existing literature lacks in a detailed study of a futuristic network with co-existing multi-RATs in mmWave networks with NOMA [7], [8]. The proposed system model investigates the coexistence of multi-RATs using uSBS tier and mSBS tier. Offloading is performed in the HetNet for load balancing.
- Offloading in the HetNet requires SBS tier to serve the OU from the MBS tier. It might not be possible to allocate an entire bandwidth to the OU at the SBS tier due to resource constraints. Hence, to support the OU, the uSBS tier and mSBS tier employs NOMA. The OU is paired with the user available at the SBS tier (called the pairing user) and served using NOMA.
- Standalone network comprising of only mSBS poses issue of large initial access delay [9], [10]. The assumption of co-located uSBS and mSBS in the proposed system model lowers the initial access delay in the mSBS. The proposed system model considers two-step association procedure where, the first step is for the tier selection, and second step is for the RAT selection. The two-step association procedure speeds up the initial access procedure, as explained in detail in Section II-B. The work in [2] discusses about the co-located multi-RAT,

This work is supported in part by the R&D project under the Visvesvaraya PhD Scheme of Ministry of Electronics and Information Technology, Government of India, being implemented by Digital India Corporation (formerly Media Lab Asia), in part by DST-UKIERI (DST/INT/UK/P-129/2016 and DST-UKIERI-2016-17-0060), and in part by the third phase of technical education quality improvement program (referred to as TEQIP-III) of Ministry of Human Resource Development (MHRD), Government of India, under the Collaborative Research Scheme.

P. Swami and V. Bhatia are with Indian Institute of Technology Indore, Indore, India; M. K. Mishra is with Samrat Ashok Technological Institute Vidisha, India, and T. Ratnarajah is with the Institute for Digital Communications, University of Edinburgh, Edinburgh, UK.

however, the system model does not consider NOMA. Further, unlike the proposed work, [2] does not consider limited feedback for user scheduling (explained in detail Section II.C of the manuscript).

- For a system with large number of users, efficiently collecting the required CSI is a challenging task, especially when the feedback links are of limited capacity. Furthermore, using network centric approach for RAT selection [11], [12] also involves exchanging significant communication overheads. The overhead is reduced by using limited feedback from the users. In the current literature, limited feedback is used only for ordering of the users [4], [7]. However, in the proposed work, unlike using limited feedback only for user ordering, the usage of limited feedback from the users is twofold. The first one is for the RAT selection (explained in Section II.B.2) and the second one is for the user scheduling (explained in Section II.C).

II. Proposed System Model for NOMA Enabled Hybrid UHF/mmWave Network

The proposed system model consists of a HetNet comprising an MBS tier, uSBS tier, and mSBS tier represented by $T = \{b, u, m\}$, respectively. The base stations (BSs) follow independent Poisson point process (PPP) based distribution, Ω_T, with density λ_T for the T^{th} tier. Offloading is performed in the HetNet for load balancing. The uSBS and mSBS are assumed to be co-located [2] (explained in Section II.B). The uSBSs are equipped with single antenna while the mSBS transmit using M antennas. Both uSBS and mSBS uses NOMA to support the enormous users. The transmit power and communication range are denoted by P_T and $\mathcal{Y}_T$, respectively, for the BS of T^{th} tier. The target data rate is denoted as R. For UHF band, bounded path loss model is considered [3], [13]. The mmWave channel model is expressed as follows [7]

$$\mathbf{h}_t^m = \frac{\sqrt{M} h_{t,0}^m \mathbf{a}(\theta_t^0)}{\sqrt{1 + (r_t^m)^{\nu_m^{LOS}}}} + \sum_{l=1}^{L} \frac{\sqrt{M} h_{t,l}^m \mathbf{a}(\theta_t^l)}{\sqrt{1 + (r_t^m)^{\nu_m^{NLOS}}}}, \quad (1)$$

where L is the number of multi-paths, and $\mathbf{a}(\bar{\theta}) = \frac{1}{\sqrt{M}} \begin{bmatrix} 1 & e^{-j\pi\bar{\theta}} & \dots & e^{-j\pi(M-1)\bar{\theta}} \end{bmatrix}^T$. The distance between the typical user (TU) and the nearest BS of the T^{th} tier is denoted by r_t^T, such that $T = \{b, u, m\}$, owing to the nearest neighbor (NN) connection policy [1], [3]. The ν_{NLOS} and ν_{LOS} denote the path loss exponents for the non-line-of-sight (NLOS) and line-of-sight (LOS) paths, respectively. The $h_{t,l}^m$ represents the complex gain for the l^{th} path and is assumed to be complex Gaussian distributed, i.e., $h_{t,l}^m \sim \mathcal{CN}(0, 1)$. The normalized direction of the l^{th} path is denoted as θ_t^l. As discussed in [7] and [14], the gain of an LOS link in mmWave communications can be 20 dB stronger than those of NLOS links. Therefore, the LOS path dominates and the simplified channel model can be written as $\mathbf{h}_t^m = \sqrt{M} \frac{h_{t,0}^m \mathbf{a}(\theta_t^0)}{\sqrt{1+(r_t^m)^{\nu_m}}}$ [7], [15], where $\nu_m = \nu_m^{LOS}$. To model the blockages, the probability that a mmWave link of distance r is an LOS path is given as $\tau(r) = e^{-\phi r}$ [7], [16], where the value of ϕ is decided by the shape, size, density, etc. of the buildings. Ignoring the correlations between the blockages, two independent non-homogeneous PPP are obtained, one for the LOS mSBSs and one for the NLOS mSBSs with respective density functions given as $\tau(r)\lambda_m$ and $(1-\tau(r))\lambda_m$. The conditional probability density function (PDF) of distance of the TU to the nearest LOS mSBS is given as [1]

$$f_{r_t^m}(r) = \frac{2\pi\lambda_m r \tau(r) e^{-2\pi\lambda_m \int_0^r x\tau(x)dx}}{B_L}, \quad (2)$$

where $r > 0$, B_L is the probability that the TU has at least one LOS mSBS and is given as $B_L = 1 - e^{-2\pi\lambda_m \int_0^\infty x\tau(x)dx}$.

A. Random Beamforming

In this work, random beamforming is used [7], [15], represented as $\mathbf{p} = \mathbf{a}(\theta)$, where θ is the normalized direction and thereby is uniformly distributed between -1 and 1. The central angle of the sector formed by the beam is 2Δ. Since, only the LOS component is considered, the superscript 0 is dropped hereafter. Following [7], [15] the effective channel gain of a user on the randomly generated beam, $|\mathbf{h}_t^*|^2 = |(\mathbf{h_t^m})^\mathbf{H}\mathbf{p}|^2$, can be expressed as follows,

$$|\mathbf{h}_t^*|^2 = |\tilde{h}|^2 \frac{\sin^2\left(\frac{\pi M(\theta-\theta_t)}{2}\right)}{M \sin^2\left(\frac{\pi(\theta-\theta_t)}{2}\right)} = |\tilde{h}|^2 F_M\left(\pi[\theta - \theta_t]\right), \quad (3)$$

where $|\tilde{h}|^2 = \frac{|h_t^m|^2}{1+(r_t^m)^{\nu_m}}$, the operator $|.|$ stands for the absolute value, and $F_M(x)$ denotes the Fejér kernel such that $F_M(x) \to 0$ for increasing x. This implies that a large effective channel gain on the beam is possible only when the user's channel vector and the direction of beam are aligned.

B. Two-Step Association Procedure

So far, the concept of biased received power (BRP) for association has been used for offloading between the tiers only (i.e., tier selection) [3], [12]. The proposed work considers BRP for tier selection and also for RAT selection using a two-step association procedure which lowers the initial access delay for the mSBS tier. In the first step, user compares the BRP from the nearest MBS with the BRP from the nearest uSBS and selects the tier with the higher BRP (explained in Section II.B.1). Hence, we are able to offload users from the MBS tier to the SBS tier. In the first step of tier selection, the uSBS can determine the location of the users using suitable signal processing techniques [17]. For standalone mSBS, providing initial access using beam-training with thin beams is a difficult task as highlighted in [2], [9]. If the position of uSBS and mSBS relative to one another are known, the users' information acquired by the uSBS in the first step can be shared with the mSBS. This speeds up the initial access procedure since the coarse-grained angle information for beamtraining can be derived easily using the shared information from the uSBS. Since, the information is shared between the uSBS and mSBS, it is termed that the uSBS and the mSBS are co-located. Later, in the second step, the user compares the BRP from the nearest uSBS with the BRP from the nearest mSBS. Based on the signal strength, the user selects whether it will associate with the uSBS or mSBS (explained in Section II.B.2). This is called as RAT selection in the proposed work. The proposed two-step association scheme is different from the scheme where the biased received powers from all the tiers and RATs are compared together (i.e., one-step procedure) [18]. However, access delay is lower when two-step association is used, as argued in [2]. This is because the users' position can be acquired using the UHF band in the first step before performing beamtraining which speeds up the initial access procedure for mSBS.

1) Step-1: Tier Selection Probability: The tier selection probability is based on the long term averaged BRP from the uSBS and MBS tier [3], [12]. The tier with higher BRP is selected by the user. The probability of a user selecting the uSBS tier is expressed as

$$\begin{aligned}\mathcal{P}_u^S &= \mathbb{E}_{r_t^u}\left[\mathcal{P}\left(B_b P_b (r_t^b)^{-\nu_b} < B_u P_u (r_t^u)^{-\nu_u}\right)\right]\\ &= \mathbb{E}_{r_t^u}\left[\mathcal{P}\left(r_t^b > \left(\frac{B_b P_b}{B_u P_u}\right)^{\frac{1}{\nu_b}} (r_t^u)^{\frac{\nu_u}{\nu_b}}\right)\right]\\ &\overset{(a)}{=} \mathbb{E}_{r_t^u}\left[\left(e^{-2\pi C_{11}} - e^{-\pi\lambda_b \mathcal{Y}_b^2}\right)\right], \end{aligned} \tag{4}$$

where (a) follows from the PDF of r_t^b, which is given as $f_{r_t^b}(r) = 2\pi\lambda_b r \exp^{-\pi\lambda_b r^2}$ owing to the NN connection policy [3], $C_{11} = \lambda_b (r_t^u)^{\frac{2\nu_u}{\nu_b}} C_1^2$, and $C_1 = \left(\frac{B_b P_b}{B_u P_u}\right)^{\frac{1}{\nu_b}}$. $\mathbb{E}[\cdot]$ denotes statistical expectation. The ν_b and ν_u denote the path loss exponents for MBS tier and uSBS tier, respectively. Taking the expectation over r_t^u such that the PDF for r_t^u is given as $f_{r_t^u}(r) = 2\pi\lambda_u r e^{-\pi\lambda_u r^2}$, the tier selection probability is calculated as

$$\mathcal{P}_u^s = 2\pi\lambda_u \times \int_0^{\mathcal{Y}_u} \left(e^{-2\pi C_{11}} - e^{-\pi\lambda_b \mathcal{Y}_b^2}\right) \times r e^{-\pi\lambda_u r^2} dr_t^u. \tag{5}$$

2) Step-2: Feedback for RAT selection: Using the proposed feedback system, for RAT selection, long term averaged BRP from the nearest uSBS and nearest mSBS is compared. The feedback bit is sent by the user over the UHF band which is shared by the co-located mSBS. The user feeds bit "0" if the BRP from the nearest uSBS is higher as compared to that received from the nearest mSBS. Likewise, the user feedback is "1" if the BRP from the nearest mSBS is higher as compared to that received from the nearest uSBS. Probability of a user selecting mSBS is expressed as,

$$\begin{aligned}\mathcal{P}_m &= \mathbb{E}_{r_t^m}\left[\mathcal{P}\left(B_u P_u (r_t^u)^{-\nu_u} < B_m P_m (r_t^m)^{-\nu_m}\right)\right]\\ &= \mathbb{E}_{r_t^m}\left[\mathcal{P}\left(r_t^u > \left(\frac{B_u P_u}{B_m P_m}\right)^{\frac{1}{\nu_u}} (r_t^m)^{\frac{\nu_m}{\nu_u}}\right)\right]\\ &\overset{(b)}{=} \mathbb{E}_{r_t^m}\left[\left(e^{-2\pi\lambda_m (r_t^m)^{\frac{2\nu_{LOS}}{\nu_u}} C_2^2} - e^{-\pi\lambda_u \mathcal{Y}_u^2}\right)\right], \end{aligned} \tag{6}$$

where $C_2 = (B_u P_u / B_m P_m)^{\frac{1}{\nu_u}}$ and (b) follows from the PDF of r_t^u. Taking the expectation over r_t^m such that the PDF for r_t^m is given in (2), the probability of a user selecting mSBS is calculated as

$$\mathcal{P}_m = \int_0^{\mathcal{Y}_m} \left(e^{-2\pi\lambda_m (r)^{\frac{2\nu_m}{\nu_u}} C_2^2} - e^{-\pi\lambda_u \mathcal{Y}_u^2}\right) f_{r_t^m}(r) dr. \tag{7}$$

Similarly, probability of user selecting uSBS is given as $\mathcal{P}_u = 1 - \mathcal{P}_m$.

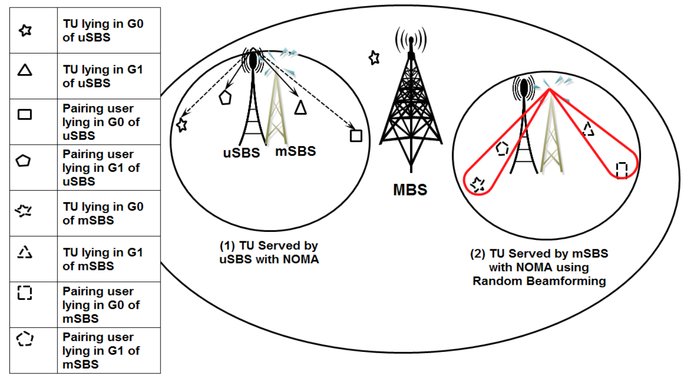

Fig. 1: Proposed System Model

C. Feedback for User Scheduling

Assuming users have perfect CSI, a user compares its fading gain to a predefined threshold broadcasted by the uSBS and mSBS, denoted by $\xi_r > 0$, such that $r \in \{u, m\}$ denotes the UHF and mmWave RAT, respectively. Given h_t^r as the channel gain at the user with respect to the r^{th} RAT, the user feeds back bit 0 if $|h_t^r|^2 < \xi_r$ and sends bit 1, otherwise. Accordingly, a user is distinguished as Group-1 (G_1^r) user of the r^{th} RAT, when bit 1 is transmitted or Group-0 (G_0^r) user of the r^{th} RAT, when bit 0 is fed [4]. For user pairing, if the OU falls in Group-0 ($G0$), it is paired up with a pairing user from Group-1 ($G1$), and vice versa (as shown in Fig. 1). Using one-bit feedback can be disadvantageous if the choice of threshold selection is poor, for instance, taking the threshold too low such that a user with poor channel is categorized as strong user or taking the threshold too high such that a strong user is categorized as a weak user. A good choice of threshold should avoid such problem. As per the existing literature in [4], [7], the optimal threshold should decrease with the SNR.

III. Signal to Interference and Noise Ratio (SINR)

A. SINR at TU: uSBS with NOMA

Given x_i as the intended signal for user in G_i^u such that $i \in \{0, 1\}$, the signal transmitted by the uSBS can be written as $X_{tx}^u = x_0\sqrt{a_0 P_u} + x_1\sqrt{a_1 P_u}$, where a_i denotes the power allocated to i^{th} group such that $a_0^2 + a_1^2 = 1$. The signal received by user in G_i^u is given by $X_{rx}^u = h_i^u X_{tx}^u + n_u$, where n_u denotes the additive white Gaussian noise (AWGN). User in G_0^u decodes its own message with the SINR,

$$\mathcal{S}_0^u = \frac{\rho_u |h_0^u|^2 a_0^2}{\rho_u |h_0^u|^2 a_1^2 + \rho_u^I I_u + \rho_b^I I_b + 1}, \tag{8}$$

where $\rho_u = \mathbb{E}[x_i^2]/\sigma_u^2$ represents the transmit signal to noise ratio (SNR) at uSBS and σ_u^2 is the noise variance[1]. $\rho_u^I = P_u/\sigma_u^2$ and $\rho_b^I = P_b/\sigma_b^2$ denotes the transmit SNR from the uSBS and MBS tier, respectively, responsible for interference. According to the Slivnyak's theorem the TU is assumed to be located at the origin [3] and let the tagged uSBS be located at u_0. Hence, the interference from the uSBS tier and MBS

[1]For MBS tier using feedback, the SINR can be written similar to that of $\mathcal{S}_1^u$, and is given as $\mathcal{S}_b = \frac{\rho_b |h_b|^2}{\rho_u^I I_u + \rho_b^I I_b + 1}$, where $\rho_b = \mathbb{E}[x_i^2]/\sigma_b^2$. The outage probability is expressed as $\mathcal{P}_b = \mathcal{P}(\log(1 + \mathcal{S}_b) < R)$.

tier at the TU is written as $\mathcal{I}_u = \sum_{i\in\Omega_u/\{u_0\}} |h_i^u|^2$, and $\mathcal{I}_b = \sum_{i\in\Omega_b} |h_j^b|^2$, where $|h_i^u|^2$ and $|h_j^b|^2$ denotes the total channel gain from i^{th} uSBS and j^{th} MBS to the TU, respectively.

User in G_1^u first performs successive interference cancellation (SIC) to decode, and remove the signal for corresponding user in G_0^u with SINR,

$$\mathcal{S}_{1\to 0}^u = \frac{\rho_u |h_1^u|^2 a_0^2}{\rho_u |h_1^u|^2 a_1^2 + \rho_u^I \mathcal{I}_u + \rho_b^I \mathcal{I}_b + 1}. \tag{9}$$

The user then decodes it own message with the following SINR

$$\mathcal{S}_1^u = \frac{\rho_u |h_1^u|^2 a_1^2}{\rho_u^I \mathcal{I}_u + \rho_b^I \mathcal{I}_b + 1}. \tag{10}$$

B. SINR at TU: mSBS with NOMA

The mSBS superimposes the signals of G_i^m, such that $i \in \{0,1\}$, on the beam as $X_{tx}^m = \mathbf{p}\left(a_0 x_0 + a_1 x_1\right)$.

The user in G_i^m receives the signal as, $X_{rx}^m = \left(\mathbf{h_i^m}\right)^H \mathbf{p}\left(a_0 x_0 + a_1 x_1\right) + n_m$, where n_m denotes the AWGN.

The user in G_0^m decodes its own message directly with the SINR,

$$\mathcal{S}_0^m = \frac{\rho_m |(\mathbf{h_0^m})^H \mathbf{p}|^2 a_0^2}{\rho_m |(\mathbf{h_0^m})^H \mathbf{p}|^2 a_1^2 + 1}. \tag{11}$$

The user in G_1^m first performs SIC with the following SINR,

$$\mathcal{S}_{1\to 0}^m = \frac{\rho_m |(\mathbf{h_1^m})^H \mathbf{p}|^2 a_0^2}{\rho_m |\mathbf{h}_1^H \mathbf{p}|^2 a_1^2 + 1}. \tag{12}$$

Then, the user decodes its own message with SINR given as,

$$\mathcal{S}_1^m = \rho_m |(\mathbf{h_1^m})^H \mathbf{p}|^2 a_1^2. \tag{13}$$

As discussed in [10], the communication in mmWave frequency is noise limited, therefore, in this work, the co-tier interference is ignored.

IV. Rate Outage Probability Analysis

1) Cumulative distribution function (CDF) of channel gain for user in G_0^u: The CDF of channel gain for uSBS tier can be expressed as

$$F_{|h_t^u|^2}(y) = \int_0^{\mathcal{Y}_u} \left(1 - e^{-(1+(r)^{\nu_u})y}\right) \times f_{r_t^u}(r) dr. \tag{14}$$

Using Gaussian-Chebyshev quadrature (GCQ) [13], (14) may be approximated as

$$F_{|h_t^u|^2}(y) \approx \sum_{n=0}^{N} b_n^u e^{-c_n^u y}, \tag{15}$$

where N is the complexity-accuracy trade-off parameter for GCQ, $b_n^u = -\pi\lambda_u \mathcal{Y}_u^2 w_N \sqrt{1-\alpha_n^2}\left(\frac{1}{2}\left(\alpha_n+1\right)\right) e^{-\pi\lambda_u\left(\frac{1}{2}(\alpha_n+1)\mathcal{Y}_u\right)^2}$, $b_0 = -\sum_{n=1}^{N} b_n^u$, $c_n^u = 1 + \left(\frac{\mathcal{Y}_u}{2}\alpha_n + \frac{\mathcal{Y}_u}{2}\right)^{\nu_u}$, $c_0 = 0$, $w_N = \frac{\pi}{N}$, $\alpha_n = \cos\left(\frac{2n-1}{2N}\pi\right)$ [13]. Using the condition to be a G0 user (as explained in Section II.C), the CDF of the channel for a user in G_0^u can be evaluated as follows:

$$F_0^u(y) = \frac{\mathcal{P}\left(|h_t^u|^2 < \min\{y, \xi_u\}\right)}{\mathcal{P}(|h_t^u|^2 < \xi_u)} = \frac{F_{|h_t^u|^2}(\min\{y, \xi_u\})}{F_{|h_t^u|^2}(\xi_u)}. \tag{16}$$

2) CDF of channel gain for user in G_1^u: Using the condition to be a G1 user (as explained in Section II.C), the CDF of the channel gain for a user in G_1^u, if $y < \xi_u$, is given as $F_1^u(y) = 0$, while, if $y > \xi_u$, it can be expressed as follows:

$$F_1^u(y) = \frac{\mathcal{P}\left(\xi_u < |h_t^u|^2 < y\right)}{\mathcal{P}\left(|h_t^u|^2 > \xi_u\right)} = \frac{F_{|h_t^u|^2}(y) - F_{|h_t^u|^2}(\xi_u)}{1 - F_{|h_t^u|^2}(\xi_u)}, \tag{17}$$

otherwise .

3) CDF of channel gain for user in G_0^m: When Δ approaches zero, the Fejér kernel is approximated as

$$F_M\left(\pi[\theta - \theta_t]\right) \approx M\left(1 - \frac{\pi^2 M^2 (\theta-\theta_t)^2}{12}\right) = F_M^a. \tag{18}$$

Hence, using (18) and polar co-ordinates, the CDF of channel gain for mSBS tier can be obtained as

$$F_{|\mathbf{h_t^*}|^2}(y) \approx \int_{\theta-\Delta}^{\theta+\Delta} \int_0^{\mathcal{Y}_m} \left(1 - e^{-\frac{y(1+r^{\nu_m})}{F_M^a}}\right) \frac{f_{r_t^m}(r)}{2\Delta} dr d\theta_t. \tag{19}$$

Similar to (16), the CDF of the channel gain of a user for $\xi_m > 0$, if it lies in G_0^m can be expressed as follows:

$$F_0^m(y) = \frac{\mathcal{P}\left(|\mathbf{h_t^*}|^2 < \min\{y, \xi_m\}\right)}{\mathcal{P}(|\mathbf{h_t^*}|^2 < \xi_m)} = \frac{F_{|\mathbf{h_t^*}|^2}(\min\{y, \xi_m\})}{F_{|\mathbf{h_t^*}|^2}(\xi_m)}. \tag{20}$$

4) CDF of channel gain for user in G_1^m: For $y < \xi_m$, $F_1^m(y) = 0$, while, if $y > \xi_m$, the CDF of the effective channel gain for user in G_1^m can be expressed similar to (17) as follows:

$$F_1^m(y) = \frac{\mathcal{P}\left(\xi_m < |\mathbf{h_t^*}|^2 < y\right)}{\mathcal{P}\left(|\mathbf{h_t^*}|^2 > \xi_m\right)} = \frac{F_{|\mathbf{h_t^*}|^2}(y) - F_{|\mathbf{h_t^*}|^2}(\xi_m)}{1 - F_{|\mathbf{h_t^*}|^2}(\xi_m)}. \tag{21}$$

A. Rate Outage Probability for uSBS Tier

The outage probability of a user in G_0^u can be expressed as $\mathcal{P}_0^u = \mathcal{P}\left(\log(1+\mathcal{S}_0^u) \le R\right) = F_0^u(y_0^u)$, where $y_0^u = \epsilon_0^u\left(1 + \rho_u^I \mathcal{I}_u + \rho_b^I \mathcal{I}_b\right)$, $\epsilon_0^u = \frac{\eta}{\rho_u\left(a_0^2 - \eta a_1^2\right)}$, $\eta = 2^R - 1$. The outage probability for $\xi_u < y_0^u$ is always equal to 1 while for $\xi_u > y_0^u$ is given as

$$\mathcal{P}_0^u = \sum_{n=0}^{N} b_n^u e^{-s_0^u} \mathcal{L}_{\mathcal{I}_u}(s_0^u \rho_u^I) \mathcal{L}_{\mathcal{I}_b}(s_0^u \rho_b^I) / \sum_{n=0}^{N} b_n^u e^{-c_n^u \xi_u}, \tag{22}$$

where $s_0^u = c_n^u \epsilon_0^u$, $\mathcal{L}_{\mathcal{I}_{T'}(s)}$ denotes the Laplace transform of the interference from T'^{th} tier such that $T' \in \{u, b\}$ and is expressed as follows:

$$\mathcal{L}_{\mathcal{I}_{T'}}(s) = \exp\left(\pi\lambda_{T'}\left(s^{\delta_{T'}}\Gamma(1-\delta_{T'}, s) - s^{\delta_{T'}}\Gamma(1-\delta_{T'})\right)\right), \tag{23}$$

where $\delta_{T'} = 2/\nu_{T'}$ such that $T' \in \{b, u\}$, $\Gamma(a, x) = \int_x^\infty t^{a-1} e^{-t}$ and $\Gamma(z) = \int_0^\infty x^{z-1} e^{-x}$. Similarly, for user in G_1^u, the outage probability can be calculated as

$$\mathcal{P}_1^u = 1 - \mathcal{P}\left(\log(1+\mathcal{S}_{1\to 0}^u) \ge R, \log(1+\mathcal{S}_1^u) \ge R\right) = F_1^u(y_1^u), \tag{24}$$

where $y_1^u = \epsilon_{max}^u\left(1 + \rho_u^I \mathcal{I}_u + \rho_b^I \mathcal{I}_b\right)$, $\epsilon_1^u = \frac{\eta}{\rho_u\left(a_1^2\right)}$ and $\epsilon_{max}^u = \max\left(\epsilon_0^u, \epsilon_1^u\right)$. The outage probability is given as

$$\mathcal{P}_1^u = \sum_{n=0}^{N} b_n e^{-s_1^u} \mathcal{L}_{\mathcal{I}_u}(s_1^u \rho_u^I) \mathcal{L}_{\mathcal{I}_b}(s_1^u \rho_b^I) - \mathcal{X}/(1-\mathcal{X}), \tag{25}$$

where $\mathcal{X} = \sum_{n=0}^{N} b_n e^{-c_n^u \xi_u}$ and $s_1^u = c_n^u \epsilon_{max}^u$.

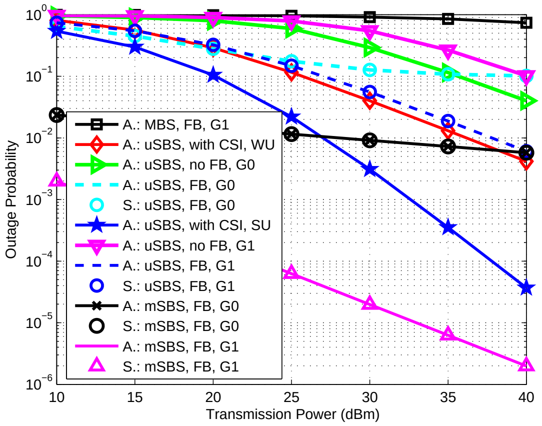

Fig. 2: Outage probability without offloading.

B. Rate Outage Probability for mSBS Tier

Similar to Section IV.A, the outage probability of user in G_0^m can be expressed as

$$\mathcal{P}_0^m = \mathcal{P}\left(\log(1+\mathcal{S}_0^m) \leq R\right) = F_0^m(y_0^m), \quad (26)$$

where $y_0^m = \epsilon_0^m$, $\epsilon_0^m = \frac{\eta}{\rho_m\left(a_0^2 - \eta a_1^2\right)}$. For user in G_1^m, the outage probability can be calculated as

$$\mathcal{P}_1^m = 1 - \mathcal{P}\left(\log(1+\mathcal{S}_{1\to0}^m) \geq R, \log(1+\mathcal{S}_1^m) \geq R\right). \quad (27)$$

This gives $\mathcal{P}_1^m = F_1^m(y_1^m)$, where $y_1^m = \epsilon_{max}^m$, $\epsilon_1^m = \frac{\eta}{\rho_m\left(a_1^2\right)}$ and $\epsilon_{\max}^m = \max\{\epsilon_0^m, \epsilon_1^m\}$.

C. Tier-Outage Probability after Offloading and RAT selection

In this section, we calculate the outage probability at each tier, i.e., at the MBS tier, uSBS tier, and mSBS tier, after offloading and RAT selection. The outage probability at the MBS tier after offloading is given as $(1-\mathcal{P}_u^s)\mathcal{P}_b$. The outage probabilities at uSBS tier and mSBS tier after offloading and RAT selection are calculated as $\mathcal{P}_u^s\mathcal{P}_u\mathcal{P}_o^u$ and $\mathcal{P}_u^s\mathcal{P}_m\mathcal{P}_o^m$, respectively.

V. Results and Discussions

This section evaluates the outage probability of the proposed feedback system in a NOMA enabled hybrid UHF/mmWave network. The system parameters considered are $\lambda_b = 10^{-5}$, $\lambda_u = 5\times10^{-4}$, $\lambda_m = 5\times10^{-3}$, $B_b = B_u = 1$, $B_m = 3$, $\mathcal{Y}_b = 1$km, $\mathcal{Y}_u = 100$m, $\nu_b = 3.5$, $\nu_u = 3$ [12], $\mathcal{Y}_m = 10$m, $\nu_m = 2$, $\Delta = 0.01$, $\phi = 0.01$, $M = 4$ [7], $R = 0.1$ bps, $N = 10$ [3], $\xi_u = \frac{1}{\rho_u}$, $\xi_m = \frac{1}{\rho_m}$ [4], [7]. For a comparative analysis, the proposed system model is compared with the following benchmarks, (i) using perfect CSI at BSs, (ii) when no offloading (off.) is performed, and (iii) when no feedback (FB) is available at the SBS from the users. Also, for comparison, users in group $G0$ and group $G1$ are considered analogous to the weak user (WU), i.e., user with poor channel gain, and the strong user (SU), i.e., user with good channel gain, respectively. Transmission power of 30 dBm is considered for comparison. The analytical results (denoted by A.) are verified using the simulation results (denoted by S.).

Fig. 2 shows the outage probability curves for the MBS tier, uSBS tier and mSBS tier without offloading. It is evident from Fig. 2 that perfect CSI at SBS provides lower bound on the outage probability. Also, since the mmWave communication is directional, it aids in reducing the interference, hence translating to lower outage probability at the mSBS tier. As it can be observed from Fig. 2, the proposed feedback system achieves lower outage probability as compared to when feedback is not available at the uSBS tier from the users. This is because, when feedback is not available, the uSBS orders the users randomly and allocates random power. Due to random power allocation, user with weak channel gain may get lower power. Hence, the outage probability deteriorates. On the other hand, the proposed feedback system distinguish the user as $G0$ user or $G1$ user, based on the feedback received by the users. This aids in appropriate power allocation to the users leading to improved outage probability by 56.97% and 90.27% for user in $G0$ and $G1$, respectively, of the uSBS tier. As the transmission power increases, the interference at $G0$ user from the signal of $G1$ user also increases. Hence, an error floor appears at high transmission power [13] for the $G0$ user, as can be observed from Fig. 2.

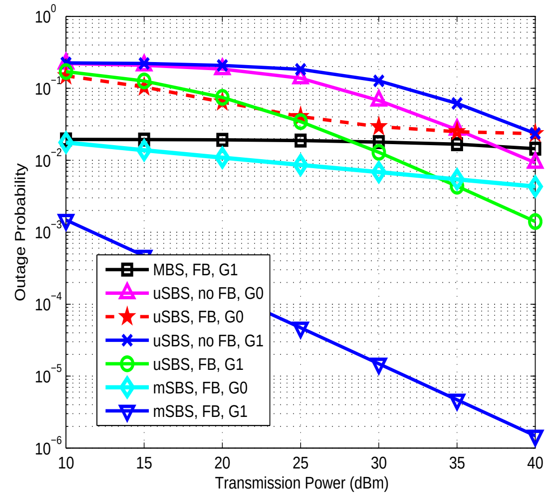

Fig. 3: Tier-outage probability with offloading and RAT selection.

Fig. 3 illustrates the tier outage probability at the MBS tier, uSBS tier, and mSBS tier after offloading and RAT selection. Compared with the no offloading scenario, offloading to uSBS/mSBS tier decreases the outage probability at the MBS tier by 98.04%. Furthermore, offloading improves the outage probability at the uSBS tier by 76.85% when offloaded as $G0$ user, and by 76.86% when offloaded as $G1$ user. Additionally, using the proposed feedback system decreases the outage probability by 56.95% and 90.26% for user offloaded in $G0$ and $G1$, respectively, as compared to offloading using no feedback. This is due to allocation of random power because of the unavailability of feedback at the SBS from the users. Moreover, the mSBS tier achieves improvement in the outage probability by 25.09% and 25.06% for user offloaded in $G0$ and $G1$, respectively, as compared to when no offloading is performed. The improvement in the tier outage probability justifies the importance of offloading in HetNets.

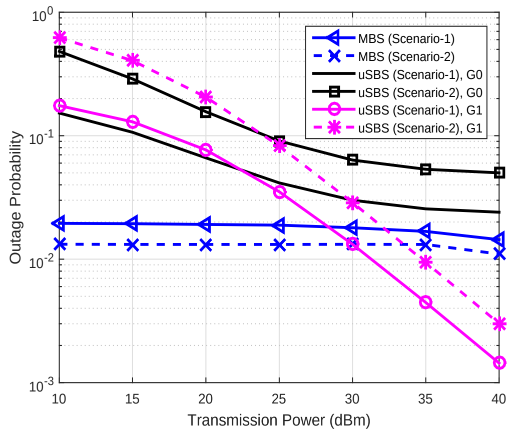

Fig. 4: Comparison of proposed work with the scenario when offloading is performed to uSBS only (with sum transmission power of $P_m + P_u$).

For a fair comparison, in Fig. 4, performance of the following two scenarios have been analyzed and compared:

1) Scenario-1: When offloading is performed using uSBS only (with sum transmit power of $P_m + P_u$.
2) Scenario-2: When proposed scheme is used wherein the offloading is performed to uSBS (with a transmission power P_u) and to mSBS (with a transmit power P_m).

It can be observed from Fig. 4 that when offloading is performed to uSBS with sum transmit power of $P_m + P_u$ (Scenario-1), the outage probability at the MBS tier improves as compared to when offloading is performed in a HetNet with uSBS (with a transmit power P_u) and mSBS (with a transmit power P_m), i.e., Scenario-2. The reason is that, in Scenario-1, the uSBS tier transmit using the sum transmit power of $P_m + P_u$, i.e., with higher as compared to the transmit power of uSBS in Scenario-2, which is only P_u. The increased power at the uSBS tier increases the offloading probability from the MBS tier to the uSBS tier (as can be observed from (4)). Increased offloading probability indicates larger number of users being offloaded from the MBS tier to the uSBS tier. This improves the outage probability at the MBS tier since the users which could experience outage when connected to the MBS tier can now be offloaded to the uSBS tier in larger number as compared to Scenario-2. However, it can be observed from Fig. 4 that the outage probability at the uSBS tier degrades. The reason is that increase in power at the uSBS increases the co-tier interference at the user, which leads to deterioration in the outage probability [19].

Hence, to accommodate the increasing number of users, increasing the power at the available base stations is not a convincing solution anymore. Considering new approaches, e.g., utilizing the frequency bands at the mmWave frequency has proven to be a promising solution for the future generation network.

VI. Conclusion

This work investigates the impact of proposed feedback system for RAT selection and user scheduling in a NOMA enabled hybrid UHF/mmWave network. When CSI is unknown at the SBS, the proposed feedback system achieves much lower outage probability in comparison to when no feedback is available from the users. Moreover, the numerical results demonstrate that offloading to multi-RAT SBS tier using the proposed feedback system improves the outage probability of the HetNet significantly.

References

[1] T. Bai and R. W. Heath, "Coverage and rate analysis for millimeter-wave cellular networks," *IEEE Trans. Wireless Commun.*, vol. 14, no. 2, pp. 1100–1114, 2015.
[2] G. Ghatak, A. De Domenico, and M. Coupechoux, "Coverage analysis and load balancing in HetNets with millimeter wave multi-RAT small cells," *IEEE Trans. Wireless Commun.*, vol. 17, no. 5, pp. 3154–3169, 2018.
[3] P. Swami, V. Bhatia, S. Vuppala, and T. Ratnarajah, "A cooperation scheme for user fairness and performance enhancement in NOMA-HCN," *IEEE Trans. Veh. Technol.*, vol. 67, no. 12, pp. 11 965–11 978, 2018.
[4] P. Xu, Y. Yuan, Z. Ding, X. Dai, and R. Schober, "On the outage performance of non-orthogonal multiple access with 1-bit feedback," *IEEE Trans. Wireless Commun.*, vol. 15, no. 10, pp. 6716–6730, 2016.
[5] X. Liu and H. Jafarkhani, "Downlink non-orthogonal multiple access with limited feedback," *IEEE Trans. Wireless Commun.*, vol. 16, no. 9, pp. 6151–6164, 2017.
[6] Q. Yang, H.-M. Wang, D. W. K. Ng, and M. H. Lee, "NOMA in downlink SDMA with limited feedback: Performance analysis and optimization," *IEEE J. Sel. Areas Commun.*, vol. 35, no. 10, pp. 2281–2294, 2017.
[7] Z. Ding, P. Fan, and H. V. Poor, "Random beamforming in millimeter-wave NOMA networks," *IEEE Access*, vol. 5, pp. 7667–7681, 2017.
[8] ——, "On the coexistence of non-orthogonal multiple access and millimeter-wave communications," in *IEEE Int. Conf. Commun. (ICC)*, 2017, pp. 1–6.
[9] Y. Li, J. G. Andrews, F. Baccelli, T. D. Novlan, and J. Zhang, "On the initial access design in millimeter wave cellular networks," in *IEEE Globecom Workshops (GC Wkshps)*, 2016, pp. 1–6.
[10] J. G. Andrews, T. Bai, M. N. Kulkarni, A. Alkhateeb, A. K. Gupta, and R. W. Heath, "Modeling and analyzing millimeter wave cellular systems," *IEEE Trans. Commun.*, vol. 65, no. 1, pp. 403–430, 2017.
[11] V. Sagar, R. Chandramouli, and K. Subbalakshmi, "Software defined access for HetNets," *IEEE Commun. Mag.*, vol. 54, no. 1, pp. 84–89, 2016.
[12] S. Singh, H. S. Dhillon, and J. G. Andrews, "Offloading in heterogeneous networks: Modeling, analysis, and design insights," *IEEE Trans. Wireless Commun.*, vol. 12, no. 5, pp. 2484–2497, 2013.
[13] Y. Liu, Z. Ding, M. Elkashlan, and J. Yuan, "Non-orthogonal multiple access in large-scale underlay cognitive radio networks," *IEEE Trans. Veh. Technol.*, vol. 65, no. 12, pp. 10152–10157, 2016.
[14] T. S. Rappaport, E. Ben-Dor, J. Murdock, and Y. Qiao, "38 GHz and 60 GHz angle-dependent propagation for cellular & peer-to-peer wireless communications." in *IEEE International Conf. Commun. (ICC)*, 2012, pp. 4568–4573.
[15] G. Lee, Y. Sung, and J. Seo, "Randomly-directional beamforming in millimeter-wave multiuser MISO downlink," *IEEE Trans. Wireless Commun.*, vol. 15, no. 2, pp. 1086–1100, 2016.
[16] T. Bai, R. Vaze, and R. W. Heath, "Analysis of blockage effects on urban cellular networks," *IEEE Trans. Wireless Commun.*, vol. 13, no. 9, pp. 5070–5083, 2014.
[17] A. Kangas and T. Wigren, "Angle of arrival localization in LTE using MIMO pre-coder index feedback," *IEEE Commun. Lett.*, vol. 17, no. 8, pp. 1584–1587, 2013.
[18] H. Elshaer, M. N. Kulkarni, F. Boccardi, J. G. Andrews, and M. Dohler, "Downlink and uplink cell association with traditional macrocells and millimeter wave small cells," *IEEE Trans. Wireless Commun.*, vol. 15, no. 9, pp. 6244–6258, 2016.
[19] J. G. Andrews, F. Baccelli, and R. K. Ganti, "A tractable approach to coverage and rate in cellular networks," *IEEE Trans. Commun.*, vol. 59, no. 11, pp. 3122–3134, 2011.